View metadata, citation and similar papers at core.ac.uk
brought to you by CORE
provided by KITopen

Simulation of a Reactor for the Partial Oxidation of o-Xylene to Phthalic Anhydride Packed with Ceramic Foam Monoliths

By A. REITZMANN, A. BAREISS and B. KRAUSHAAR-CZARNETZKI*

Abstract

The potential of ceramic foams as fixed bed catalyst carriers in the partial oxidation of o-xylene to phthalic anhydride was evaluated by means of numerical simulations. One- and two-dimensional, pseudo-homogeneous reactor models were used to compare the performances of fixed bed reactors filled with foam packings and with spherical catalyst bodies, both of which coated with the same catalyst. The results show that foam packings enable a highly selective and more efficient operation of PA reactors. The improved heat transfer properties, higher specific surface areas and higher porosities of foam packings allow for a stretching of the operational window to more severe process conditions while the danger of catalyst deactivation and thermal runaways is reduced. The results indicate that the space-time-yield of phthalic anhydride could be more than doubled, if conventional fixed beds of catalyst particles would be replaced by foam packings.

1 Introduction

Ceramic foam monoliths are open-cell materials with a sponge-like structure. Ceramic struts form an irregular, three-dimensional network. The void volume can be visualised as a stack of cages, so-called cells, which are interconnected through windows in all directions (Fig. 1). These materials can be used as monolithic packings with high void volumes in the range of $\varepsilon = 0.7–0.9$, and with high geometric surface areas per volume packing of up to 10,000 m^2/m^3. Ceramic foams are commonly applied as filters for molten metals [1] and can be made in a large variety of compositions [2].

Several aspects make these materials to promising candidates for structured catalyst carriers [1, 3].

– The open structure leads to a considerably reduced pressure drop as compared to packed beds of catalyst bodies with the same geometric surface area [4, 5].
– In contrast to honeycomb monoliths, characterised by parallel, separated channels and laminar flow inside, foams enable a turbulent flow in all directions.
– Literature data indicate that heat and mass transfer is improved in ceramic foams as compared to beds of catalyst bodies. Heat, in particular, is transferred more efficiently due to considerable contributions of conduction through the foam struts, and of radiation at temperatures above 400°C [6, 7].

Since ceramic foam monoliths apparently combine properties of packed beds and honeycombs in a beneficial way, several applications as catalyst carriers have been suggested [3, 6], however, only a few have been evaluated in more detail so far [8–11].

The present study focuses on the evaluation of a foam-packed reactor to be used in the heterogeneously catalysed, partial oxidation of o-xylene to phthalic anhydride (PA). In the industrial processes, multi-tubular, fixed bed reactors (> 20,000 tubes per reactor) are commonly used. Today, these are filled with shaped bodies, spheres, rings or hollow cylinders, coated with a 100–200 µm thin layer of V_2O_5/TiO_2 catalysts ("egg-shell") to avoid internal mass transfer limitations. The process is characterised by high rates of all reactions and a pronounced exothermicity ($\Delta H_{R,av} \sim 1500$ kJ/mol). Insufficient heat removal causes pronounced axial temperature gradients across the catalyst bed. If the operating conditions slightly change, the risk of a thermal reactor runaway is given [12]. In addition, temperatures above 500°C accelerate an irreversible deactivation of the catalyst [13]. For these reasons and because of the high pressure drop over the bed of catalyst bodies, industrial PA-reactors must be operated at lower o-xylene inlet concentrations and lower temperatures than would be desirable to obtain high PA space-time-yields.

In this article, we describe reactor simulations using pseudo homogeneous models which were carried out to compare fixed bed PA reactors filled either with ceramic foam monoliths or with catalyst particles. It was our aim to find out whether the substitution of conventional fixed beds by catalytically coated ceramic foams might be a suitable means to overcome the above-mentioned restrictions in the performance of PA reactors.

2 Models and Correlations for Reactor Simulation

2.1 One-dimensional model

In the first step, a one-dimensional, pseudo-homogeneous reactor model was used, assuming plug-flow behaviour, constant volume, velocity and pressure, and equal bed porosity at all locations. These simplifications were made because there are only a few reliable data and correlations available so far to describe flow and heat transfer in foam structures at the conditions of the PA process [6, 7, 14, 15]. However, recent estimations concerning the residence time distributions in foam-packed reactors have shown that under conditions, similar to those in PA reactors, axial dispersion can be neglected and

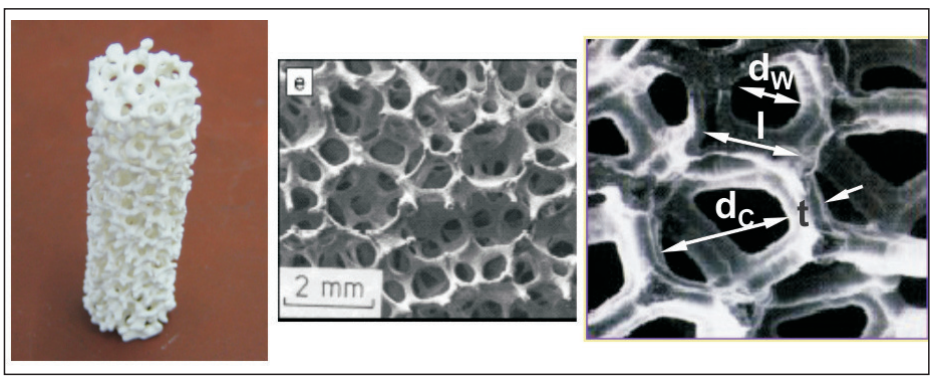

Fig. 1 Structure and morphology of ceramic foams (d_C: cell diameter, d_W: window diameter, t: strut thickness, l: strut length)

*A. Reitzmann, A. Bareiss, B. Kraushaar-Czarnetzki, Institute of Chemical Process Engineering CVT, University of Karlsruhe (TH), 76128 Karlsruhe, Germany. Lecture presented at the DGMK/SCI Conference „Oxidation and Functionalization: Classical and Alternative Routes and Sources", October 12–14, 2005, Milan, Italy (E-mail: Andreas.Reitzmann@ciw.uni-karlsruhe.de)

0179-3187/06/II
© 2006 URBAN-VERLAG Hamburg/Wien GmbH

EVA-STAR (Elektronisches Volltextarchiv – Scientific Articles Repository)
http://digbib.ubka.uni-karlsruhe.de/volltexte/1000004584

Table 1 **Parameters for Eqs. (4) and (5) [15]**

Material	Pore density (ppi)	a	b	c	K_{rad}	$\lambda_{rad}^{eff\,1)}$, W m^{-1}K^{-1}
Cordierite	20	0.79	$-3.65\cdot10^{-3}$	$4.50\cdot10^{-6}$	2.60	3.36
SiC	10	–0.56	$2.40\cdot10^{-3}$	$5.00\cdot10^{-7}$	3.07	5.67
	20	–0.20	$2.40\cdot10^{-3}$	0	1.60	6.33
	45	1.20	$-3.90\cdot10^{-3}$	$1.10\cdot10^{-5}$	0.90	7.51

1) T = 350 °C

Table 2 **Typical features of industrial PA production, and simulation conditions (= base case for spheres and foams)**

Parameter	Industrial Conditions [12, 17, 19]	Simulation Conditions
tube inner diameter, mm	25	25
tube length, m	3–3.5	2.8
catalyst bed length, m	2.8	2.8
flow rate per tube, Nm^3·h^{-1}	3–4.5	4
o-xylene feed concentration, kg·Nm^{-3}	60–105	80
pressure, 10^5 Pa	~ ambient	1.5 average
inlet reactor temp., °C	~250	250
coolant (= wall) temp., °C	340–380	348
catalyst dimensions	6 mm (spheres) 8 x 5 x 5 mm (rings)	6 mm (spheres) 20 ppi (foams)
bed porosity	0.40–0.60	0.4 (spheres) 0.8 (foams)
pressure drop, 10^5 Pa m^{-1}	~ 0.18 (rings)	0.313 (spheres) 0.218 (foams)[1)]
surface area per reactor volume, m^{-1}	not available	600 (spheres) 2550 (foams)[2)]
mass of active catalyst per reactor volume, kg m^{-3}	70–100	100

1) calculated according to [4]; 2) calculated according to $S_V = 4\cdot\varepsilon/d_p$ [5]

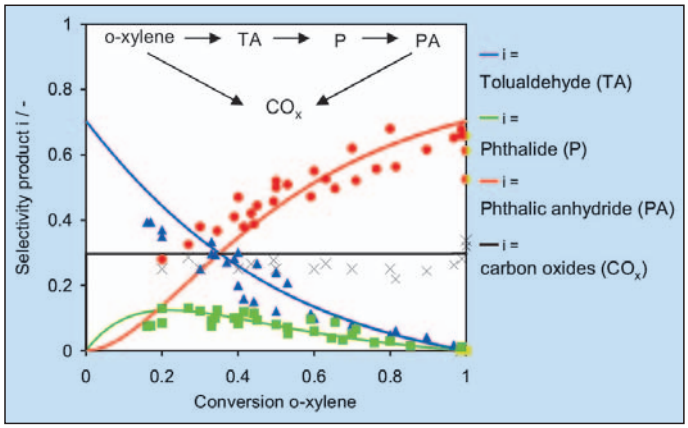

Fig. 2 **Reaction kinetics of o-xylene oxidation: product selectivities versus o-xylene conversion and reaction network (symbols: literature data [20, 21]; lines: kinetic model; 360 °C)**

plug-flow behaviour can, indeed, be assumed [10]. The model equations necessary for the modelling a single tube of the multitubular fixed bed reactor are the *mass balance:*

$$\frac{dx_i}{dz} = \left[\frac{1}{\dot{n}_{total}}\right]\cdot\rho_{cat}\cdot A_c\cdot R_i \qquad (1)$$

and the *energy balance*:

$$\frac{dT}{dz} = -\frac{4U^{eff}(T-T_W)}{d_t G_0 C_P} + \frac{\rho_{cat}}{G_0 C_P}\sum_j^{n_R}\left(-\Delta H_r\right)_j\cdot r_j \qquad (2)$$

Boundary conditions are:

$$x_i(z=0) = x_{i,0};\ T(z=0) = T_0$$

The overall heat transfer coefficient (U^{eff}) was calculated according to

$$\frac{1}{U^{eff}} = \frac{1}{\alpha_W} + \frac{d_t}{8\cdot\lambda_{rad}^{eff}} \qquad (3)$$

This implies that heat transfer resistances in the tube wall and from the tube to the coolant, commonly a salt bath, were neglected. The parameter α_w represents the heat transfer through a highly porous region of the catalyst bed at the inner reactor wall, and λ_{rad}^{eff} denotes the effective radial heat conductivity. For the simulation of the reactor filled with a fixed bed of particles, the values of α_w and λ_{rad}^{eff} in eq. 3 were determined using correlations for heat transfer given in [16]. However, these correlations have not been developed for foams but rather for packings of shaped particles. For α_w in foams, in particular, there exist no data, so far. We estimated the value of α_w for foams by means of the correlation in [16], thereby representing the foam as a bed of spheres with the same specific surface area per bed volume. Our calculation of the value of λ_{rad}^{eff} is based on eqs. (4) and (5) below, and on the parameters listed in Table 1 for cordierite, all of which taken from a study by Decker et al. [14, 15]. There, various ceramic foams were used as porous burners, and heat transfer was investigated for flow conditions very similar to those in PA reactors.

Effective radial conductivity:

$$\lambda_{rad}^{eff} = \lambda_0 + \frac{G_0 c_p d_p}{K_{rad}} \qquad (4)$$

Stagnant bed conductivity:

$$\lambda_0 = a + b\cdot T + c\cdot T^2 \qquad (5)$$

2.2 Two-dimensional model

The one-dimensional model might be sufficient to show general trends. However, in strongly exothermic processes like the PA synthesis, radial temperature gradients significantly affect the reactor performance [17]. In order to show these gradients, a two-dimensional, pseudo-homogeneous approach was applied in the second step. The $\Lambda_r(r)$-model, described in detail in [18], was chosen to circumvent any problems with weak correlations for the parameter α_w. Neglecting axial mass and heat dispersion as in the one-dimensional model, these balance equations were used:

mass balance

$$0 = -u(r)\frac{M_i}{M_t}\frac{\partial(x_i)}{\partial z} + \frac{1}{r}\frac{\partial}{\partial}\frac{M_i}{M_t}\left(rD_{rad,i}^{eff}(r)\frac{\partial x_i}{\partial r}\right) + \frac{M_i}{\rho_f}\cdot\frac{1-\varepsilon(r)}{1-\varepsilon_\infty}\rho_{cat}\cdot R_i \qquad (6)$$

and *energy balance*

$$0 = -\rho_F C_p u(r)\frac{\partial T}{\partial z} + \frac{1}{r}\frac{\partial}{\partial r}\left(r\lambda_{rad}^{eff}(r)\frac{\partial T}{\partial r}\right) + \frac{1-\varepsilon(r)}{1-\varepsilon_\infty}\rho_{cat}\cdot\sum_{j=1}^{N_j}(\Delta_R H_j)\cdot r_j \qquad (7)$$

The following boundary conditions are valid:

$$T(r=R) = T_W,\qquad \left.\frac{\partial x_i}{\partial r}\right|_{r=R} = 0 \qquad (8)$$

$$T(z=0) = T_0,\qquad x_i(z=0) = x_{i,0} \qquad (9)$$

$$\left.\frac{\partial T}{\partial z}\right|_{z=L} = 0,\qquad \left.\frac{\partial x_i}{\partial z}\right|_{z=L} = 0 \qquad (10)$$

$$\left.\frac{\partial T}{\partial z}\right|_{r=0} = 0,\qquad \left.\frac{\partial x_i}{\partial z}\right|_{r=0} = 0 \qquad (11)$$

In the case of the bed of spheres, the change of the porosity across the radius reactor was described with eq. (12).

$$\varepsilon(r) = \varepsilon_\infty\cdot\left[1+1.36\cdot\exp\left\{-5\cdot\left(\frac{\frac{d_t}{2}-r}{d_p}\right)\right\}\right] \qquad (12)$$

The value 0.4 was chosen for the porosity ε_∞ in the centre of the fixed bed. The momentum balance is based on the extended Brinkman equation

$$\frac{\partial p}{\partial z} = -f_1 u(r) - f_2 u(r)^2 + \frac{\eta_{eff}}{r}\frac{\partial}{\partial r}\left(r\frac{\partial u}{\partial r}\right) \qquad (13)$$

and yields a velocity profile. Correlations for the friction factors, f_1 and f_2, as well as for

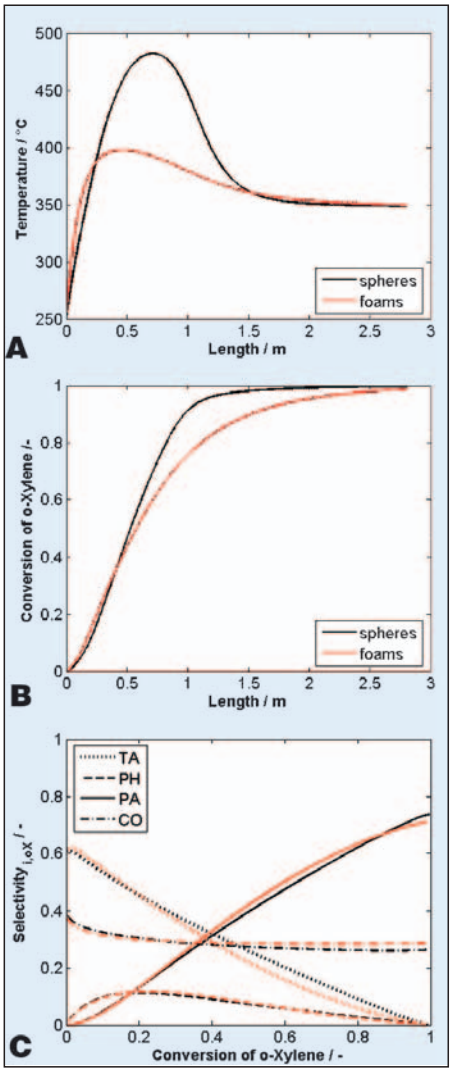

Fig. 3 Calculated performances of fixed beds of cordierite foams (base case) and spheres in the oxidation of o-xylene to PA; (A) temperature profile and (B) o-xylene conversion versus reactor length, (C) product selectivities versus o-xylene conversion. Conditions are summarised in Table 2 (TA: o-tolualdehyde, PH: phthalide, PA: phthalic anhydride, CO: carbon monoxide)

the effective viscosity accounting for the wall friction, η_{eff}, are given in [18]. Correlations for calulating the effective radial transfer parameters were taken from [16, 18].

For a fixed bed consisting of spherical particles, this model is well established and proven [18]. However, neither any porosity profile nor an extended Brinkmann equation is available for foam packings. In order to provide a reasonable comparison between spheres and foams, the foam packing was simulated with the same model, thereby, however, implementing the radial heat transfer parameters according to eqs. (4) and (5), and using the data in Table 1 for cordierite.

2.3. Kinetics

Reaction network and kinetic parameters of the partial oxidation of o-xylene to PA were taken from [17, 19]. With the resulting kinetic model, data from isothermal experiments [20, 21] as shown in Figure 2 as well as measured temperature profiles in non-isothermal reactors ([17]) can be described satisfactorily for the purpose of this study.

2.4 Operational conditions

Table 2 summarises the bed features and process conditions assumed for the reactor simulations. The values were chosen such that industrial operation is closely approximated.

Two differences between the fixed beds consisting of spheres and of foam should already be emphasized at this point:

– The pressure drop along the foam is lower than along the bed of spheres
– The spheres must be coated with a much thicker layer of catalyst (about 145 µm) than the foam (about 34 µm) to ensure the same intake of catalyst mass per unit volume (here: 100 kg/m^3(Reactor), assumed catalyst bulk density: 1150 kg/m^3 (V_2O_5/TiO_2)). This is a consequence of the diverging specific surface areas of the two carrier types. Although the pseudo-homogeneous model used for our simulations does not take into account internal mass transfer limitations, these might have a negative effect in particle beds or, vice versa, mass transfer limitations can be avoided much better when foam packings are used.

3 Results and Discussion

3.1. Comparison of reactors packed with cordierite spheres and foams (one-dimensional model)

Figure 3A shows axial temperature profiles calculated with the one-dimensional model. In the foam packing, the hot-spot temperature is significantly reduced. In addition, the position of the temperature maximum is shifted to the reactor inlet due to the improved heat transfer in the foam. As a consequence of the lower average temperature in the foam packing, full conversion of o-xylene requires a higher bed length (Fig. 3B). At technically relevant conversion levels above ca. 90%, the PA selectivity is lower and CO selectivity is higher for the foam packing (Fig. 3C) resulting slightly less PA space-time-yield.

These "base case" results show that the good heat transfer in combination with the high surface area and the low pressure drop in foam packings opens several options for an increase in the PA space-time-yield. These options will be addressed in the following case studies.

3.2 Influence of the operational conditions on the performance of reactors packed with foam (case studies)

3.2.1 Catalyst intake and total flow

In this case study, we increased the thickness of the catalyst layer on the foam packing. The hot spot temperature of the sphere packing, 482 °C, was regarded as the upper limit for reactor operation. Using a foam packing,

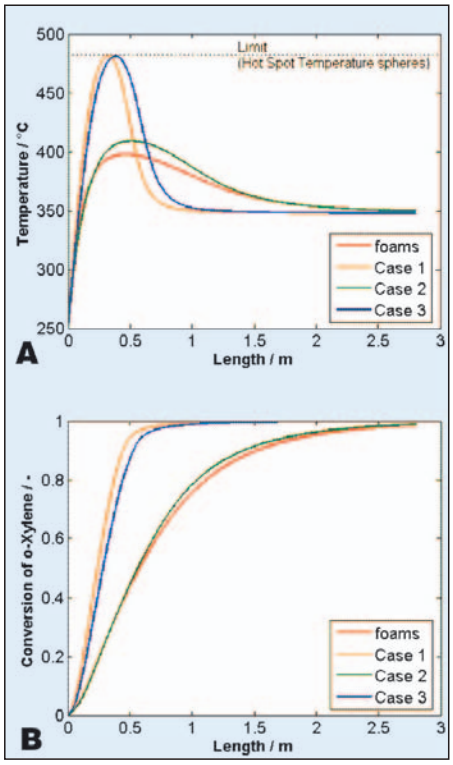

Fig. 4 Temperature profile (A) and o-xylene conversion (B) versus reactor length in a foam packing; cases are explained in Table 3

this hot spot temperature would be reached with a catalyst intake of 220 kg/m^3, which is equivalent to a layer thickness of 75 µm (Fig. 4A, case 1). This change results in increases in the o-xylene conversion, the PA selectivity and in the space-time-yield (Fig 4B and Table 3, case 1) as compared to the "base case". The performance of the fixed bed of spheres, however, is not exceeded.

The lower pressure drop of the foams offers the possibility to increase the total flow by a factor of about 1.24 as compared to the bed of spheres. If the ratio of catalyst loading and total flow is kept constant (Fig. 4 and Tab. 3, case 2), the hot spot temperature is reduced. Conversion and PA selectivity are lower than over the bed of spheres, but the PA space-time-yield is considerably enhanced because of the larger throughput.

Since the higher flow rate improves the rate of heat removal, the amount of catalyst can be further increased up to 230 kg/m^3 until the hot spot temperature of the sphere packing is reached (Fig. 4 and Tab. 3, case 3). In this case 3, a slightly higher PA selectivity and yield, but particularly a higher space-time-yield of 307 $kg_{PA} \cdot m^{-3} \cdot h^{-1}$ than for the sphere packing can be achieved.

3.2.1 Feed composition and coolant temperature

The improved heat transfer in foams also offers possibilities to enhance the feed concentration of o-xylene, and to reduce the temperature of the coolant. In the investigation of these options (cases 4 to 6, Table 4), the hot spot temperature of the fixed bed of

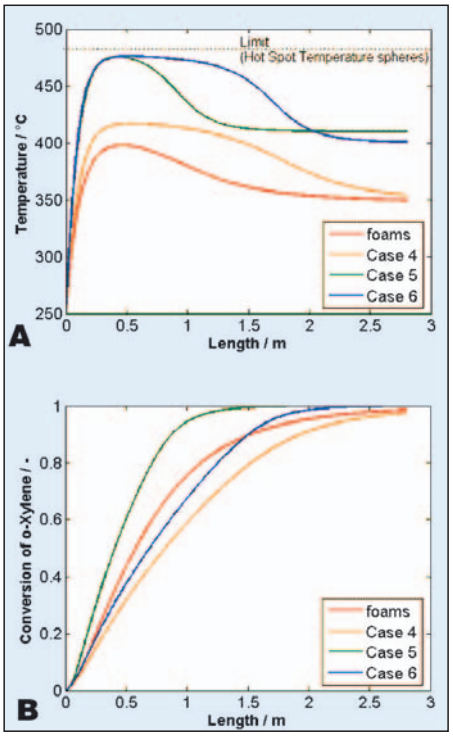

Fig. 5 **Temperature profile (A) and o-xylene conversion (B) versus reactor length in a foam packing; cases are explained in Table 4**

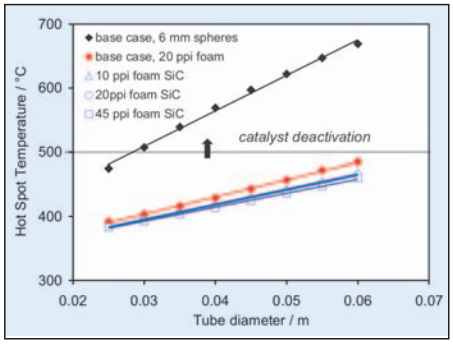

Fig. 6 **Influence of the tube diameter on the hot spot temperature; the horizontal black line indicates the temperature limit, above which typical PA catalysts are irreversibly deactivated**

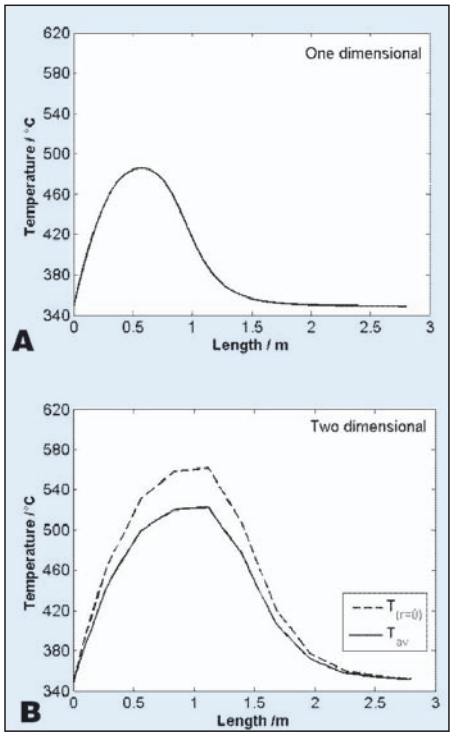

Fig. 7 **Comparison of axial temperature profiles in the fixed bed of spheres obtained with (A) one- and (B) two-dimensional models (here: $T_0 = T_W = 348$ °C)**

spheres (482 °C) was again regarded as a limit for the reactor operation.

In the fist step, the inlet concentration of o-xylene was increased from 80 g/m_N^3 (base case) to 175 g/m_N^3 (case 4). By this operation, the hot spot temperature is raised, but still remains considerably below the upper limit (Fig. 5A). In spite of the higher average temperature as compared to the base case, the conversion of o-xylene (Fig. 5B) is reduced. The reason for this behaviour is the fact that o-xylene has an inhibiting effect on the reaction rate, i. e. the rate equation for o-xylene has an order smaller than unitiy in the concentration of o-xylene [17]. Nevertheless, case 4 allows for a considerable increase in the space-time-yield of PA because of the higher throughput (Tab. 4).

Back to the original inlet concentration of 80 g/m_N^3, case 5 represents a situation in which the temperature of the coolant (= wall) is increased from 348 °C to 410 °C. Now, reactor temperature and o-xylene conversion are strongly enhanced (Fig. 5A and B), and the achievable space-time-yield of PA can be increased.

Finally, the beneficial effects of higher wall temperature and feed concentration were combined. Both parameters were increased as far as a o-xylene conversion of at least 99% was achieved at the reactor exit without exceeding the upper limit of the hot spot temperature. These conditions were met with a o-xylene feed concentration of 175 g/m_N^3 and a wall temperature of 410 °C (case 6). Through these changes in operation, the PA selectivity can be further increased, and the achievable space-time-yield amounts to more than the double as compared to a reactor with a fixed bed of spheres.

3.3 Tube dimensions in a multi-tubular reactor

The costs for construction and operation of multi-tubular PA reactors can be reduced considerably, if tubes with larger diameters could be installed. Our simulations show that this is, indeed, an option, if the conventional particle beds are replaced by foam packings. The results depicted in Figure 6 refer to the base cases for foams and spheres as described in Table 2. They indicate that the tube diameter may at least be doubled upon substitution with foam carriers made of cordierite. The hot spot temperatures can be further reduced by a value of up to 15 °C, if SiC foams are applied instead of cordierite, because these exhibit better heat transfer properties (Table 1).

3.4 Results of two-dimensional modelling

The two dimensional model was used in order to visualise the radial temperature profiles in the tubular reactors. It is important to notice, however, that allowing for a radial temperature distribution also has an effect on the axial temperature profile. This is shown in Figure 7 for the fixed bed of spheres. The two-dimensional model calculates not only a higher hot spot temperature at the centre of the pipe ($T_{r=0}$), but also a higher average value for a cross section (T_{av}). On the other hand, the conversions and selectivities (not shown) calculated with both models are very close, confirming that the one-dimensional model is suitable to establish reliable trends.

Figure 8 shows the two-dimensional temperature distributions in fixed beds of spheres and foams under the same operational conditions (base cases in Table 2, but with $T_0 = T_W$). It becomes obvious that the radial gradients are much lower in the foam than in the sphere packing, resulting in a much more

Table 3 **Quantitative comparison of sphere and foam packings, and the effects of catalyst loading and total flow rate (foam)**

Case	ρ_{cat}, $kg_{cat}.m^{-3}$	Flow rate, $Nm^3\,h^{-1}$	$T_{HotSpot}$, °C	STY, $kg_{PA}\,m^{-3}h^{-1}$	S_{PA}, [1)]	Y_{PA}, [1)]
Spheres	100	4	482	247	0.74	0.73
Base case foams	100	4	398	235	0.71	0.70
Case 1	220	4	482	247	0.74	0.74
Case 2	124	4.94	409	295	0.71	0.71
Case 3	230	4.94	481	307	0.74	0.74

[1)] molar values (mol/mol)

Table 4 **Quantitative comparison of sphere and foam packings, and the effects of xylene concentration and coolant temperature (foam)**

Case	T_{wall}, °C	$T_{HotSpot}$, °C	$C_{0,o\text{-}xylene}$, $g\,m_N^{-3}$	STY, $kg_{PA}\,m^{-3}h^{-1}$	S_{PA}, [1)]	Y_{PA}, [1)]
Spheres	348	482	80	247	0.74	0.73
Base case foams	348	398	80	235	0.71	0.70
Case 4	348	417	175	512	0.72	0.70
Case 5	410	476	80	249	0.74	0.74
Case 6	400	476	175	545	0.75	0.75

[1)] molar values (mol/mol)

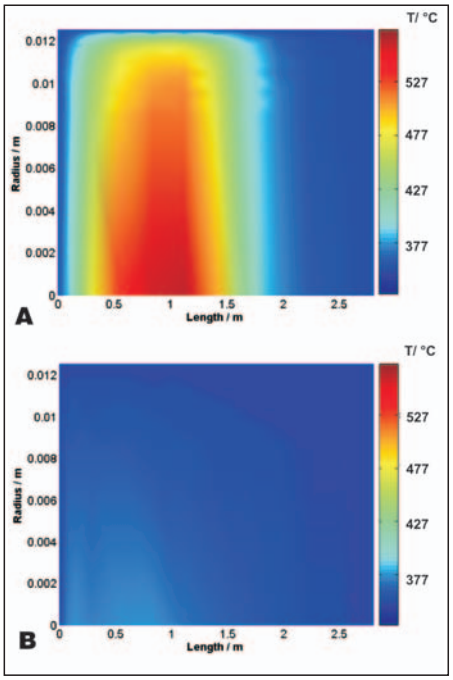

Fig. 8 **Temperature field in a fixed bed PA reactor consisting of (A) spheres and (B) of a foam packing**

homogeneous temperature profile in axial and radial direction.

4 Conclusions

The reactor simulations show the potential of ceramic foams as a catalyst packing in fixed bed reactors for the partial oxidation of o-xylene to phthalic anhydride. Improved heat transfer properties, higher surface areas and higher porosities of ceramic foam packings enable a highly selective and more efficient operation as compared to fixed beds of spherical catalyst bodies. The results indicate that the space-time-yield of phthalic anhydride could be more than doubled. The danger of catalyst deactivation and thermal runaways can be reduced because a more homogeneous temperature field can be realised within the foam bed.

The simulations were performed with one- and two-dimensional reactor models. In the case of fixed beds of spheres, the calculations could be based on validated correlations for fluid dynamics and heat transfer. So far, most of these correlations are lacking for foam packings, and some non-validated assumptions had to be made. Being aware of this weakness, we still believe that the simulations provide reliable trends and give valuable insights in the performance of reactors packed with catalytically coated foam.

Symbols

A_c/m^2	area cross-section of tube
c_p/J kg^{-1}K^{-1}	specific heat capacity
d_p/m	sphere diameter, mean pore diameter
d_t/m	tube diameter
G_0/kg m^{-2}s^{-1}	superficial mass velocity
K_{rad}/-	radial slope parameter
r_j/mol m^{-3}s^{-1}	rate of reaction j
r/m	radial coordinate
R_i/mol m^{-3}s^{-1}	molar consumption rate of species i ($=\sum(\nu_{i,j}\cdot r_j)$)
S_V/m^{-1}	foam surface area per reactor volume
u/m s^{-1}	superficial velocity
T_W/K	wall temperature = coolant temperature
U^{eff}/W m^{-2}K^{-1}	eff. overall heat transfer coefficient
x_i/-	molar fraction of species i
z/m	axial coordinate
α_w/W m^{-2}K^{-1}	wall heat transfer coefficient
ε/-	bed porosity
ε_∞/-	bed porosity without wall effects
λ_{rad}^{eff}/W m^{-1}K^{-1}	effective radial heat conductivity
λ_0/W m^{-1}K^{-1}	stagnant heat conductivity
η_f/Pa s	dynamic viscosity of fluid
η_{eff}/Pa s	effective viscosity (wall friction)
ρ_{cat}/kg m^{-3}	mass of active catalyst per reactor volume
ρ_f/kg m^{-3}	fluid density
$(\Delta_R H)_j$/J mol^{-1}	enthalpy of reaction j
Re/-	Reynolds number ($=\frac{\bar{u}\cdot d_p\cdot\rho_f}{\eta_f}$)

References

[1] Twigg, M. V., Richardson, J. T., Trans IChemE 80 (2002) 183.
[2] Buciuman, F. C., Kraushaar-Czarnetzki, B., Ind. Eng. Chem. Res. 42 (2003) 1863.
[3] Twigg, M. V., Richardson, J. T., Stud. Surf. Sci. Catal 91, (1995) 345.
[4] Moreira, E. A., Innocentini, M. D. M., Coury, J. R., J. Eur. Ceram. Soc. 24 (2004) 3209.
[5] Richardson, J. T., Peng, Y., Remue, D., Appl. Catal. A:, 204 (2000) 19.
[6] Richardson, J. T., Remue, D., Hung, J.-K., Appl. Catal. A: 250 (2003) 319.
[7] Peng, Y., Richardson, J. T., Appl. Catal. A: 266 (2004) 235.
[8] Bodke, A. S., Bharadway, S. S., Schmidt, L. D., J. Catal. 179 (1998) 138.
[9] Fino, D., Saracco, G., Specchia, V., Chem Eng. Sci. 57, (2002) 4955.
[10] Donsi, F., Cimino, S., Di Benedetto, A., Pirone, R., Russo, G., Catal. Today 105 (2005) 551.
[11] Patcas, F. C., J. Catal. 231 (2005) 194.
[12] Anastasov, A. I., Chem. Eng. J. 86 (2002) 287.
[13] Anastasov, A. I., Chem. Eng. Process. 42 (2003) 449.
[14] Decker, S., Mößbauer, S., Nemoda, S., Trimis, D., Zapf, T., in: 6th International Conference on Technologies and Combustion for a Clean Environment (Clean Air VI) Porto, Portugal, 9–12 July 2001, Vol. 2 (2001) 22.2.
[15] Decker, S., Durst, F., Trimis, D., Nemoda, S., Stamatov, V., Steven, M., Becker, M., Fend, T., Hoffschmidt, B., Reutter, O., final report DFG project DU 101/55-1 (2002).
[16] VDI-Wärmeatlas, 9th ed., Springer Verlag (2002) and enclosed references.
[17] Anastasov, A. I., Chem. Eng. Sci. 58 (2003) 89.
[18] Winterberg, M., Tsotsas, E., Krischke, A., Vortmeyer, D., Chem. Eng. Sci. 55 (2000) 967.
[19] Boger, T., Menegola, M., Ind. Eng. Chem. Res. 44 (2005) 30.
[20] Skrzypek, J., Grzesik, M., Galantowicz, M., Solinski, J., Chem. Eng. Sci. 40 (1985) 611.
[21] Papageorgiou, N., Abello, M.C., Froment, G. F., Appl. Catal. A: 120 (1994) 17.

Andreas Reitzmann *studied chemical engineering at the University of Erlangen -Nürnberg where he did his PHD thesis in 2001. Since this time he is working in the function of an assistant professor at the Institute of Chemical Process Engineering at the university of Karlsruhe (TH). His present research interests are devoted to reaction engineering of catalytic, partial oxidations.*

Anika Bareiss *studied Process Engineering at the University of Karlsruhe (TH) until 2003. Since this time, she is PHD student at the Institute of Chemical Process Engineering at the university of Karlsruhe (TH). Her topic is the "Partial oxidation of o-xylene in fixed bed reactors packed with foam catalysts".*

Bettina Kraushaar-Czarnetzki *is head of the Institute of Chemical Process Engineering at the University of Karlsruhe since 1996. She studied Chemistry and Chemical Engineering, and holds a PhD from Eindhoven University of Technology. From 1989 till 1996, she was employee of Shell Research BV. Her present research activities are devoted to catalytic multiphase reaction engineering.*